Improving Efficiency of Large Time-Scale Molecular Dynamics Simulations of Hydrogen-Rich Systems

K. ANTON FEENSTRA, BERK HESS, HERMAN J. C. BERENDSEN

Bioson Research Institute and Laboratory of Biophysical Chemistry, University of Groningen, Nijenborgh 4 9747 AG Groningen, The Netherlands

Received 19 October 1998; accepted 15 January 1999

ABSTRACT: A systematic analysis is performed on the effectiveness of removing degrees of freedom from hydrogen atoms and/or increasing hydrogen masses to increase the efficiency of molecular dynamics simulations of hydrogen-rich systems such as proteins in water. In proteins, high-frequency bond-angle vibrations involving hydrogen atoms limit the time step to 3 fs, which is already a factor of 1.5 beyond the commonly used time step of 2 fs. Removing these degrees of freedom from the system by constructing hydrogen atoms as dummy atoms, allows the time step to be increased to 7 fs, a factor of 3.5 compared with 2 fs. Additionally, a gain in simulation stability can be achieved by increasing the masses of hydrogen atoms with remaining degrees of freedom from 1 to 4 u. Increasing hydrogen mass without removing the high-frequency degrees of freedom allows the time step to be increased only to 4 fs, a factor of two, compared with 2 fs. The net gain in efficiency of sampling configurational space may be up to 15% lower than expected from the increase in time step due to the increase in viscosity and decrease in diffusion constant. In principle, introducing dummy atoms and increasing hydrogen mass do not influence thermodynamical properties of the system and dynamical properties are shown to be influenced only to a moderate degree. Comparing the maximum time step attainable with these methods (7 fs) to the time step of 2 fs that is routinely used in simulation, and taking into account the increase in viscosity and decrease in diffusion constant, we can say that a net gain in simulation efficiency of a factor of 3 to 3.5 can be achieved.
J Comput Chem 20: 786–798, 1999

Keywords: molecular dynamics; water simulation; protein simulation; time step optimization; accuracy of integration; large time-scale dynamics; constraints

Correspondence to: H. J. C. Berendsen
Contract/grant sponsors: The Netherlands Foundation for Chemical Research (SON); Foundation for Life Sciences (SLW); The Netherlands Organization for Scientific Research (NWO)

CCC 0192-8651 / 99 / 080786-13

Introduction

The maximum time step in molecular dynamics (MD) simulations is limited by the smallest oscillation period that can be found in the simulated system. Bond-stretching vibrations are the fastest atomic motions in a molecule, typically in the order of 10 fs. A classical treatment of these motions is not correct because such vibrations are in their quantum-mechanical ground state. For a proper treatment quantum-mechanical calculations should be included. It stands to reason, therefore, that for normal (classical) MD these motions are ignored altogether (i.e., they can be better represented by a constraint).

For the remaining degrees of freedom, the shortest oscillation period as measured from a simulation is 13 fs for bond-angle vibrations involving hydrogen atoms (Table I). Taking as a guideline that, with a Verlet (leap-frog) integration scheme, a minimum of five numerical integration steps should be performed per period of harmonic oscillation, in order to integrate it with reasonable accuracy,[1] the maximum time step will be about 3 fs. This is slightly larger than the 2 fs routinely used in MD simulations of biomolecules in water. Disregarding these very fast oscillations of period 13 fs (which are also in the quantum-mechanical ground state) the next shortest periods are around 20 fs, which will allow a maximum time step of about 4 fs. In simulations with constrained bond lengths and angles, it has recently been shown that hydrogen atom dihedral angle motions (e.g., rotation of hydroxyl groups) impose a 5-fs limit on the time step, whereas nonhydrogen atomic collisions (Lennard–Jones ''rattling'') restrict the time step to a maximum of 10 fs.[2]

The fastest motions in a simulation will invariably involve hydrogen atoms, because these are by far the lightest atoms present in all biological systems. The biologically relevant behavior of these systems take place mostly on large time scales—at least several nanoseconds, but often seconds, or even beyond. On these time scales hardly any influence can be expected from the tens of femtoseconds-long oscillations of hydrogen atoms.

The obvious solution would be to constrain all bond angles involving hydrogen atoms in all molecules, in addition to all bond lengths. With the SHAKE constraint algorithm[3] this can already be done, but SHAKE tends to break down with time steps beyond 2 fs. The generally more robust and faster LINCS constraint algorithm[4] is now preferred over SHAKE,[5] but cannot handle the highly connected constraints that arise from constraining both bonds and angles.[4] The most elegant solution would be to eliminate these high-frequency degrees of freedom from the system altogether.

For hydrogen atoms in large molecules (e.g., proteins) this can be implemented in a rather

TABLE I.
Characteristic Oscillation Periods of Atomic Motions in MD Simulations.[a]

Motion	f_c (kJ mol^{-1})	I (u nm^2)	Period (fs)	
			Calc.	Sim.
Bond stretch, H	400 000	m = 1 u	10	10
Bond stretch, heavy atoms	500 000	m = 12 u	30	20
Water libration	—	0.0059	—	28
Water rotation	—	0.0059	—	1300
Angle, H	375	0.010	32	20
Angle, heavy atoms	450	0.27	154	45
Angle —NH_3^+ group, C—N—H	375	0.010	32	22
Angle —NH_3^+ group, H—N—H	750	0.010	23	13
Improper, planar	167	—	—	28
Improper, tetrahedrical	335	—	—	27
Dihedral, peptide bond	33	0.20	489	28
Dihedral, —NH_3^+ group	3.8	0.023	489	89
Dihedral, OH group	1.3	0.0094	53	43

[a] f_c: force constant; I: moment of inertia, or atomic mass for bond stretching; calc.: calculated from eq. (1); sim.: highest frequency significant peak in spectrum of angle respectively dihedral motion from simulation. An entry of ''—'' means not applicable, or not determinable.

straightforward manner. Instead of connecting a hydrogen atom with bonds, angles, and dihedrals to the molecule, the position of the hydrogen will be generated every MD step based on the position of three nearby heavy atoms. All forces acting on the hydrogen atom will be redistributed over these heavy atoms. A particle treated in this manner is referred to as a *dummy atom*.[6,7] To keep the total mass in the system constant, the mass of each hydrogen atom that is treated in this way should be added to the bonded heavy atom. Care should be taken that for groups with internal rotation (e.g., hydroxyl or amine groups) only the other internal degrees of freedom of the group should be fixed, but the rotational freedom should remain.

A special case is the movement of water molecules. The internal geometries of the popular water models are already rigid, so the high-frequency motions are, in this case, librational motions of the whole water molecule. The only way these motions can be slowed down is by increasing the moments of inertia of the water molecule. This can be done best by increasing the mass of the hydrogen atoms while decreasing the mass of the oxygen atoms, such that the total mass will remain unchanged. A similar modification can be made for groups with internal rotational freedom, as hydroxyl or amine groups, which will display motional frequencies close to those of water. All this, of course, constitutes a nontrivial deviation from ''physical reality'' and requires justification.

The equilibrium distribution of a system of particles that behaves according to classical statistical mechanics (as in MD) is not dependent on the masses of the individual particles. This is not strictly true if constraints are present, due to the mass dependence of the metric tensor correction, but these corrections are usually zero or negligible. Therefore, we are at liberty to choose appropriate masses without affecting thermodynamic properties.

This idea was originally proposed by Jacucci and Rahman at a CECAM workshop in 1974,[8] and has been investigated in some detail since[6,9,10] and used in our laboratory before.[11] None of these studies contains a thorough theoretical analysis of the effects of altered masses. Moreover, those investigators who have used a systematic approach have not kept the total mass of the system constant and have failed to notice that this in fact scales system time. This is most pronounced in Mao et al.[12] who reported simulations at 600 K and normal time steps with all masses uniformly increased by a factor of 10, but who actually simulated normal masses with a $\sqrt{10}$ times smaller time step at 6000 K. This increase in system temperature accounted for all of the improved conformational sampling that was reported. Also, the approach, as outlined, has not been applied to simulations of biological (macro)molecules, which require additional modifications.

The issue is, again, time scales that are of interest for the study of biological systems. On these time scales, at least several nanoseconds, the properties of the water will average and the influence of water on the dynamics of the system is exerted through its bulk properties, like diffusion constant, viscosity, and dielectric relaxation time. Hydrogen motions in proteins are almost uncoupled from the main chain vibrations and will therefore hardly influence the behavior of the system on these time scales.

Methods

MD SIMULATIONS

All MD simulations were performed using the following parameters and methods, unless stated otherwise. The Verlet integration scheme (leapfrog) was used.[13] The GROMOS-87 force field[14] was used, with increased repulsion between water oxygen and carbon atoms.[15] Explicit hydrogens were defined for the aromatic rings; the resulting parameter set is the one referred to as SW by Daura et al.[16] Periodic boundary conditions with a rectangular box were applied. LINCS[4] was used to constrain all covalent bonds in nonwater molecules. The SETTLE algorithm was used to constrain bond lengths and angles in the water molecules.[17] The temperature was controlled using weak coupling to a bath[19] of 300 K with a time constant of 0.1 ps. Protein and water were independently coupled to the heat bath. Initial velocities were randomly generated from a Maxwell distribution at 300 K, in accordance with the masses assigned to the atoms. The pressure was also controlled using weak coupling with a time constant of 1.0 ps.

The starting conformation for the water simulations was generated by equilibrating 820 SPC (simple point charge) water molecules[20] in a 3.2-nm cubic box for 100 ps at 300 K and 1 bar, using a time step of 2 fs, and other parameters as stated earlier. Subsequently, the masses were reassigned (see Table II), and an additional equilibration was done for 10 ps using the same parameters. The

TABLE II.
Atomic Masses in Water.[a]

Mass (u)		I	η	D	$\tau_{H\ bond}$	Drift E_{tot}	Δt_{max}
H	O	(u nm^2)	(10^{-4} kg m^{-1} s^{-1})	(10^{-9} m^2 s^{-1})	(ps)	(kJ mol^{-1} ps^{-1})	(fs)
1	16	0.0059	4.3	4.08	0.67	1.04	6.6
2	14	0.0104	4.7	3.89	0.74	0.86	8.9
3	12	0.0133	4.9	3.79	0.89	0.42	10.0
4	10	0.0148	4.9	3.34	0.79	0.36	10.3
5	8	0.0148	5.1	3.50	0.84	0.47	10.4
6	6	0.0133	5.3	3.35	0.84	0.59	8.6
7	4	0.0104	5.2	3.34	0.88	0.43	7.5
8	2	0.0059	5.1	3.60	0.95	0.61	5.6
Real H_2O		—	8.0	2.3	0.59	—	—
Real D_2O		—	—	2.0	—	—	—

[a] I: corresponding smallest moments of inertia; resulting dynamical properties: η: viscosity; D: diffusion constant. Values of H_2O and D_2O from Lide et al.[33] and hydrogen-bond lifetime ($\tau_{H\ bond}$) value of H_2O from Montrose[31]; RMS drift of the total energy over 12 runs at a time step of 4 fs; maximum time step (Δt_{max}) at a maximum order of 10 of the drift as a function of time step.

same procedure was applied to a smaller (1.9-nm) cubic box containing 216 SPC water molecules and an elongated box of $1.9 \times 1.9 \times 5.6$ nm containing 648 SPC water molecules. The resulting conformations for each hydrogen mass and box shapes and sizes were used as a starting conformation for all simulations of water.

Short simulations of 1 ps starting from the equilibrated water structures of the small box of 216 SPC waters for each set of atomic masses were performed to determine the total energy drift as function of atomic mass and time step. Time steps of 0.5 to 15 fs were used; simulations with larger time steps were not stable. A shift function[21] was applied for Coulomb and Lennard–Jones interactions, which decreases the potential over the whole region and lets potential and force decay smoothly to zero between 0.5 and 0.75 nm. This introduces some artifacts into the simulation,[21,22] but it effectively removes noise from cutoff effects, enabling an accurate assessment of the simulation accuracy as determined by the time step. Neighbor list generation was performed every time step to exclude possible errors from diffusion of particles in between neighbor list updates. No pressure coupling was applied, instead the system was equilibrated to the right pressure and density and subsequently simulated at constant volume. No temperature coupling was applied.

Longer simulations of 100 ps starting from the equilibrated water structures for each set of atomic masses were performed to determine the dynamical properties of water; that is, diffusion constant, lifetime of hydrogen bonds, and viscosity. For determination of the viscosity the elongated box of 648 SPC waters was used. For the other determinations the cubic box of 820 SPC waters was used. A time step of 2 fs was used. A twin-range cutoff for nonbonded interactions was employed with a short-range cutoff for Lennard–Jones and Coulomb interactions of 0.9 nm, which were calculated every simulation step, and a long-range cutoff of 1.1 nm for Coulomb interactions, which were calculated during neighbor-list generation at every 10th step (20 fs). Neighbor searching was done based on the centers of geometry of the water molecules.[18] This is the same parameter set as was used by Van der Spoel et al.[23]

The simulations of a protein were performed with the small protein HPr (NMR PDB entry 1HDN[24]). This 85-residue α/β protein consists of a four-stranded antiparallel β-sheet flanked on one side by three antiparallel α-helices. The protein was solvated by generating a cubic box of SPC water molecules, such that the minimum distance between the protein and the edge of the periodic box would be 0.6 nm, resulting in a cubic box of 4.7 nm. All water molecules from the generated box of water that were within 0.23 nm of a protein atom were removed, leaving 2985 water molecules around the protein. The resulting conformation was energy minimized with harmonic constraints on the atomic coordinates of the protein. Subsequently, a round of 10 ps of MD was performed, also with harmonic constraints on the atomic coordinates of the protein to relax the water orientation near the protein. The final conformation was used as starting conformation for simulations of the

protein in water. Additionally, another 10 ps of MD was performed starting from this conformation. From these two final conformations the water was removed and the protein was allowed to relax for 1 ps in a vacuum environment. The final conformations from both 1-ps vacuum simulations were used as starting conformations for simulations of the protein in vacuum.

Short simulations of 1 ps of the protein in vacuum were performed to determine the total energy drift as function of time step. Four different topology types were used: the normal topology (''normal 1 u''); with the hydrogen atoms increased fourfold in mass (''normal 4 u''); with dummy hydrogens (''dummy 1 u''); and with dummy hydrogens and remaining hydrogens fourfold increased in mass (''dummy 4 u''). Time steps of 0.5 to 7 fs were used; simulations with larger time steps were not stable. No cutoff for Lennard–Jones or Coulomb interactions was applied and no periodic boundary conditions were used. No temperature coupling was applied. Although simulations of a protein in vacuum are generally not relevant for the majority of applications, these simulations do allow for a relatively accurate estimate of the energy drift, which is not possible for a simulation of the protein in water. Distortions of the shape of the protein by the vacuum environment might influence energy drift, but are unlikely to occur within the 1-ps duration of the simulations.

Long simulations of 1 ns of the protein in water were performed to determine the long-term properties of a protein using the ''normal 1 u,'' ''normal 4 u,'' ''dummy 1 u,'' and ''dummy 4 u'' topologies, with time steps ranging from 1 to 7 fs. Long-range Coulomb interactions were calculated using PPPM[25,26] with a grid spacing of 0.09 nm. Neighbor list generation was performed every 10 time steps. No pressure coupling was applied, instead the system was equilibrated to the right pressure and density and subsequently simulated at constant volume, resulting in average system pressures ranging from 14 to 80 bar, with an average of 44 bar. Within this range of pressures, no influence is likely to exist on the properties of the protein.

All MD simulations were carried out using the GROMACS molecular dynamics package[27,28] on a Silicon Graphics (SGI) Power Challenge with MIPS R10000 processors and on SGI O2 Workstations with MIPS R5000 processors. CPU times for the long (1 ns) runs of the protein in water on the SGI Power Challenge machine are summarized in Table III, for a total of 130 days of CPU time.

SYSTEM TOPOLOGY

Normal topologies, with constraints on all bonds and no constraints on angles, were generated using standard GROMACS topology building tools. These tools were modified to optionally produce the modified topologies containing the dummy atoms and remove all bond, angle, and dihedral

TABLE III.
Summary of Long (1-ns) Simulations of Protein in Water for Simulations with ''Normal 1 u,'' ''Normal 4 u,'' ''Dummy 1 u,'' and ''Dummy 4 u,'' Topologies.[a]

Δt	N_{steps}	CPU time	RMS deviation (nm)				Sec. Struct. (%)				No. of H Bonds			
			Normal		Dummy		Normal		Dummy		Normal		Dummy	
(fs)	($\times 10^3$)	(hs)	1 u	4 u	1 u	4 u	1 u	4 u	1 u	4 u	1 u	4 u	1 u	4 u
1	1000	341	0.11	0.12	0.18	0.11	87	86	85	84	114	112	117	114
2	500	171	0.15	0.15	0.17	0.13	86	85	87	85	114	111	116	118
3	333	114	0.15	0.09	0.17	0.13	87	87	82	86	114	115	114	116
4	250	86	—	0.16	0.15	0.14	—	87	85	86	—	114	116	114
5	200	68	—	—	0.12	0.16	—	—	87	85	—	—	116	114
6	167	57	—	—	0.13	0.15	—	—	88	85	—	—	117	118
7	143	49	—	—	0.11	0.18	—	—	89	84	—	—	113	116

[a] Simulation parameters: time step; number of steps; total run time on an SGI Power Challenge with MIPS R10000 processors, averaged over the four topology types. Long-term average properties: RMS deviation of all backbone atoms with respect to the starting structure, averaged over the last 100 ps; secondary structure content (% of residues not in random-coil conformation, according to the DSSP program[34]) averaged over 100 to 1000 ps; number of interprotein hydrogen bonds averaged over 100 to 1000 ps. Entries of ''—'' indicate failure of the simulation to run without errors, which was also the case for time steps larger than 7 fs.

definitions that have become obsolete due to the introduction of the dummy atoms. Also, optionally, masses of all remaining normal hydrogen atoms can be increased by a factor of four, while subtracting this increase from the bonded heavy atom. More details are included in the following section.

Construction of Dummy Atoms

The goal of defining hydrogen atoms as dummy atoms is to remove all high-frequency degrees of freedom from them. In some cases, not all degrees of freedom of a hydrogen atom should be removed (e.g., in the case of hydroxyl or amine groups the rotational freedom of the hydrogen atom(s) should be preserved). Care should be taken that no unwanted correlations are introduced by the construction of dummy atoms; for example, bond-angle vibration between the constructing atoms could translate into hydrogen bond-length vibration. Additionally, because dummy atoms are, by definition, massless, in order to preserve total system mass, the mass of each hydrogen atom treated as a dummy atom should be added to the bonded heavy atom.

All forces acting on the dummy atoms must be redistributed over the constructing atoms.[7] Dummy atom positions can be calculated easily from any three atoms that have a fixed orientation with respect to each other. If the constructing atoms move significantly with respect to each other, normalized vectors will have to be used to ensure the right position for the dummy atom. This results in complicated derivatives in the force redistribution, which are described in detail in the Appendix.

Taking into account these considerations, the hydrogen atoms in a protein naturally fall into one of several categories, each requiring a different approach (see Fig. 1):

- *Hydroxyl* (—OH) *or sulfhydryl* (—SH) *hydrogen*. The only internal degree of freedom in a hydroxyl group that can be constrained is the bending of the C—O—H angle. This angle is fixed by defining an additional bond of appropriate length (Fig. 1A). This removes the high-frequency angle bending, but leaves the dihedral rotational freedom. The same goes for a sulfhydryl group. Note that, in these cases, the hydrogen is not treated as a dummy atom.

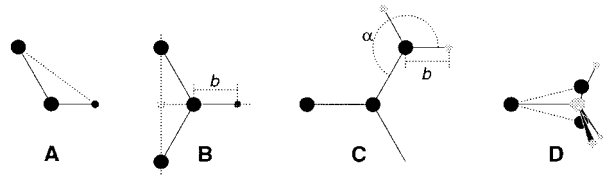

FIGURE 1. Schematic view of the different types of dummy atom constructions used. The atoms used in the construction of the dummy atom(s) are depicted as black circles, dummy atoms as gray circles. Hydrogens are smaller than heavy atoms. (A) Fixed bond angle. Note that here the hydrogen is not a dummy atom. (B) In the plane of three atoms, with fixed distance. (C) In the plane of three atoms, with fixed angle and distance. (D) Construction for amine groups (—NH_2 or —NH_3^+). See text for details.

- *Single amine or amide* (—NH—) *and aromatic hydrogens* (—CH—). The position of these hydrogens cannot be constructed from a linear combination of bond vectors, because of the flexibility of the angle between the heavy atoms. Instead, the hydrogen atom is positioned at a fixed distance from the bonded heavy atom on a line going through the bonded heavy atom and a point on the line through both second bonded atoms (Fig. 1B).
- *Planar amine* (—NH_2) *hydrogens*. The method used for the single amide hydrogen is not well suited for planar amine groups, because no suitable two heavy atoms can be found to define the direction of the hydrogen atoms. Instead, the hydrogen is constructed at a fixed distance from the nitrogen atom, with a fixed angle to the carbon atom, in the plane defined by one of the other heavy atoms (Fig. 1C).
- *Amine group* (*umbrella* —NH_2 or —NH_3^+) *hydrogens*. Amine hydrogens with rotational freedom cannot be constructed as dummy atoms from the heavy atoms they are connected to, because this would result in loss of the rotational freedom of the amine group. To preserve the rotational freedom while removing the hydrogen-bond-angle degrees of freedom, two ''dummy masses'' are constructed with the same total mass, moment of inertia (for rotation around the C—N bond), and center of mass as the amine group. These dummy masses have no interaction with any other atom, except for the fact that they are connected to the carbon and to each other, resulting in a rigid trian-

gle. From these three particles, the positions of the nitrogen and hydrogen atoms are constructed as linear combinations of the two carbon-mass vectors and their outer product, resulting in an amine group with rotational freedom intact, but without other internal degrees of freedom (Fig, 1D).

Additionally, all bonds, angles, and dihedrals that are defined on one of the degrees of freedom that were removed are also removed. This boils down to removing all bonds to dummy atoms, all angles that involve two or three dummy atoms, and all dihedrals that involve at least one dummy atom and for which all other atoms are used in constructing the dummy atom(s). Note that this leaves the whole force field unchanged.

As a second option, all remaining hydrogen atoms (i.e., in hydroxyl, sulfhydryl, amine groups, and water) can be increased in mass, with the increase subtracted from the bonded heavy atom. This leaves the total mass constant, but increases the moment of inertia of the group, effectively slowing down the motions. For the dummy mass and dummy atom construction of the amine group (type D as described earlier), this will have the net result of the dummy masses being placed further apart in accordance with the desired increase in moment of inertia.

It should be noted that in the GROMOS-87 force field aliphatic hydrogens are implicit; that is, they are represented as united C—H atoms. For an all-atom force field with all hydrogen atoms explicit, an additional number of hydrogen dummy atoms will have to be constructed every time step; for instance, for the 85-residue protein, 165 hydrogen atoms are present in the GROMOS-87 force field, but an additional 488 aliphatic hydrogens are implicit. Constructing the 165 hydrogen dummy atoms takes far less than 0.1% of the total computer time, so constructing 653 hydrogen dummy atoms will still have no noticeable effect on the total cost of simulating.

DETERMINATION OF SYSTEM PROPERTIES

Motional Periods

Periods of oscillation were measured from a simulation of the protein in water with a time step of 0.5 fs, by taking the highest frequency significant peak from the spectrum of the motion. Periods were also calculated from the force field parameters using:

$$T = 2\pi \left(\frac{I}{f_c} \right)^{1/2} \tag{1}$$

where I is the moment of inertia, determined by bond lengths and masses, and f_c the force constant of the corresponding angle or dihedral potential. Eq. (1) neglects effects of coupling with the surroundings.

Energy Drift

As outlined earlier, the simulations used to determine the drift in total energy of the simulated system were performed with neither temperature nor pressure coupling. For the water box, a shifted potential for electrostatic and Lennard–Jones interactions was used to eliminate cutoff effects and, for the protein, no cutoff for interactions was used. This was done to minimize as much as possible all sources of integration errors (notably cutoff effects), except for those caused by the ratio between time step and fastest motional periods. Also, double-precision (8 bytes) floating-point calculations were used during the simulation. The limited accuracy of summing up millions of interactions in single precision gives rise to additional drift that obscures the effects we intend to investigate, especially in the smaller time-step regime. As a measure of the accuracy, the root-mean-square (RMS) averaged drift in the total energy obtained from a least-squares linear fit over the last 0.9 ps of 1-ps simulations was used.[1]

Because the drift in the total energy of a well-integrated system is diffusive in nature, an appreciable number of independent simulations needs to be performed to get an accurate estimate of this drift. The root-mean-square drift provides a reliable measure for the accuracy of the simulation. For the water box, 12 simulations were performed for each time-step/mass combination, each with a different random seed to generate initial velocities. For the protein, two different starting conformations were used, for which six simulations with different random seeds were performed for each time-step/topology-type combination. This adds up to 1440 1-ps simulations of the water box, for a total of 12.4 hours of CPU time on a MIPS R10000 processor, and 560 1-ps simulations for the protein, for a total of 5.4 hours of CPU time.

The fluctuation of the total energy, which can be determined easily from a single simulation, is an inappropriate measure to assess the simulation accuracy of a Verlet-type (leap-frog) integration scheme, because it is of second order in time step, whereas the drift is of second to third order.[1]

Diffusion Constant

Diffusion constants (D) for water were calculated from the mean square displacement (MSD) of the water molecules using the Einstein relation for diffusion in three dimensions[29]:

$$\langle \|\mathbf{r}(t) - \mathbf{r}(0)\|^2 \rangle = 6Dt \tag{2}$$

D was determined by a linear fit to the plot of the MSD vs. time.

Viscosity

The procedure for determination of the viscosity was modified after Berendsen.[30] Viscosity was determined in a nonequilibrium simulation setup where an external shear-stress acceleration field was applied:

$$a_{i,x} = A\cos\left(\frac{2\pi z_i}{l_z}\right) \tag{3}$$

with $a_{i,x}$ being the acceleration in the x direction, A the acceleration amplitude, z_i the z-coordinate of the particle, l_z the length of the box in the z-direction. Application of this shear-stress acceleration gradient induces a velocity gradient of the same shape. For a Newtonian fluid, the dynamic viscosity, η, is given as the the ratio between the applied acceleration amplitude, A, and the resulting velocity amplitude, V[30]:

$$\eta = \frac{A}{V}\rho\left(\frac{l_z}{2\pi}\right)^2 \tag{4}$$

where ρ is the density and l_z the box length in the z-direction of the system.

The scaling procedure used in temperature coupling was modified to exclude the induced velocity gradient while applying temperature scaling.

Care was taken to choose the acceleration amplitude low enough to prevent the appearance of ordering in the water and high enough to get a velocity gradient that is discernible over the thermal velocities. An amplitude of 0.07 nm ps^{-2} was found to perform best (E. Apol, personal communications); this results in a velocity amplitude of the order of 0.1 nm ps^{-1}, which corresponds to roughly 10% of the root-mean-square thermal velocity at 300 K, which is 1.1 nm ps^{-1}. For the same reason, the acceleration field was applied along the longest edge (three times the length of the other edges) of the rectangular simulation box.

The velocity, V, amplitude was calculated using a spatial Fourier component[30]:

$$V = \frac{2}{N}\sum_i v_{i,x}\cos\left(\frac{2\pi z_i}{l_z}\right) \tag{5}$$

which was stored at every time step. The viscosity was calculated from eq. (4), using the average velocity amplitude over the last 90 ps of the simulations to exclude the equilibrational part in which buildup of the velocity gradient still occurs.

Lifetime of Hydrogen Bonds

Hydrogen bonds between water molecules were defined using a simple angle and distance criterion (i.e., angle hydrogen donor–acceptor $\leq 60°$ and distance donor–acceptor ≤ 0.35 nm), yielding a switch function of 1 when a hydrogen bond is present, and 0 otherwise. The hydrogen-bond lifetime is determined as the half-life time of the autocorrelation of the switch function.

Results

WATER

Energy Drift

In Figure 2A, the energy drift is plotted as a function of hydrogen mass and time step. Note that, for clarity, the graphs for the 2-, 3-, 6-, and 7-fs time steps are not shown (they all lie in between the plotted graphs). The drift as a function of time step is of second order, which lies within the expected range of second to third order.[1] At time steps of > 7 fs for the 1- and 8-u simulations and > 10 fs for the 4- and 5-u simulations, a transition occurs from second to higher order.

Taking a rather arbitrary value of 10 as a maximum for the order of the drift as a function of the time step, a maximum time step can be determined for each hydrogen mass. As summarized in Table II, these time steps correspond to the sharp increase in the slope of the plots in Figure 2A. For

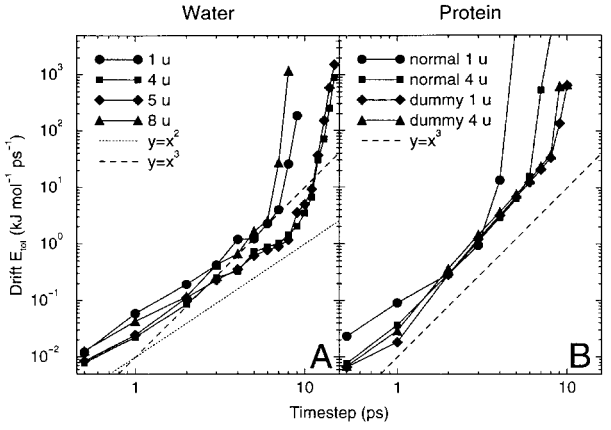

FIGURE 2. RMS averaged drift in the total energy as a function of time step of: (A) a box of SPC water (648 atoms) with different hydrogen masses (graphs for 2, 3, 6, and 7 u are omitted for clarity); (B) a small protein (805 atoms) with different topology types (''normal 1 u,'' ''normal 4 u,'' ''dummy 1 u,'' and ''dummy 4 u'').

water with the normal mass distribution, the maximum time step is 6.6 fs. The largest attainable time step of 10.4 fs occurs with water with a hydrogen mass of 5 u, an increase of a factor of 1.6. According to eq. (1), this is consistent with the increase in moment of inertia of a factor of 2.5. This correspondence is a clear indication that the librational frequency of (SPC) water is the major factor determining the maximum possible time step for accurate integration. Alternatively, a maximum for the magnitude of the drift could be chosen to determine maximum time steps; however, these data would be rather inconsistent due to the large fluctuation present in the magnitude of the drift. The very sharp increase in the order of the drift allows for a much more accurate determination of maximum time steps.

Diffusion

The diffusion constant as determined from the simulations for different atomic masses ranges from $4.1 \cdot 10^{-9}$ m^2 s^{-1} at a hydrogen mass of 1 u to $3.3 \cdot 10^{-9}$ m^2 s^{-1} at a mass of 4 u, or a decrease by a factor of 1.2 (see Table II). Compared with the difference between diffusion constants of SPC water ($4.1 \cdot 10^{-9}$ m^2 s^{-1}) and real water ($2.3 \cdot 10^{-9}$ m^2 s^{-1}), a difference of a factor of 1.8, the variation caused by changing the hydrogen mass is relatively small.

Viscosity

Viscosity for different atomic masses ranges from $4.3 \cdot 10^{-4}$ kg m^{-1} s^{-1} at a hydrogen mass of 1 u to $5.3 \cdot 10^{-4}$ kg m^{-1} s^{-1} at a mass of 6 u. At a mass of 4 u, which yields the highest maximum time step, the viscosity is $4.9 \cdot 10^{-4}$ kg m^{-1} s^{-1}, an increase of a factor of 1.1 (see Table II). Compared with the difference between the viscosity of SPC water ($4.3 \cdot 10^{-4}$ kg m^{-1} s^{-1}) and real water ($8.0 \cdot 10^{-4}$ kg m^{-1} s^{-1}), a factor of 1.9, the variation caused by changing the hydrogen mass is small. Still, the result can be significant in the sense that large-scale consorted motions in the simulation (e.g., domain motions of proteins), will be limited by the viscosity of water, which means that a higher viscosity of water will result in slower protein motion. It can be expected that the maximum slowing down will be of similar order as the increase in the viscosity of the water (i.e., about 14%).

Hydrogen Bond Lifetime

The hydrogen bond lifetime increases monotonically with the hydrogen mass, from 0.67 ps at a mass of 1 u to 0.95 ps at 8 u (see Table II), when the single deviating value at 3 u is ignored. At a hydrogen mass of 4 u, the lifetime is 0.79 ps, which is an increase by a factor of 1.2 with respect to the value of normal SPC water. The lifetime of hydrogen bonds in normal SPC water (0.67 ps) may be compared with an experimental estimate of 0.59 ps,[31] on the basis of fluctuations in the anisotropy of molecular polarizability, as determined from depolarized Rayleigh scattering measurements.

PROTEIN

Energy Drift

In Table IV, a summary is given of the results of the protein simulations (see also Fig. 2B). For time steps of 1 fs and below, the drift is diffusive in nature, as was the case for the water box, which gives rise to relatively large variations in the determined drift. For larger time steps, the drift becomes systematic and is always positive. The order of the drift as a function of time step also lies within the theoretically expected range of second to third order. Surprisingly, the magnitude of the drift is virtually identical for all topology types, and the only difference between them is the time

TABLE IV.
Summary of Maximum Time Steps (Δt_{max}).

Topology type	Δt_{max} (fs) A[a]	B[b]
Normal 1 u	3	3
Normal 4 u	6	4
Dummy 1 u	8	7
Dummy 4 u	8	7

[a] Drift of the total energy as a function of the time step in short (1-ps) simulations is still of third order.
[b] Long (1-ns) simulations can be performed without errors.

step at which a transition from third to higher order occurs. These transition time steps are summarized in Table IV (col. A).

Long-Term Properties

From Table III it is immediately obvious that the average RMS deviation from the starting structure in the last 100 ps of each run with respect to the starting structure, the secondary structure content in the last 900 ps, and the average total number of hydrogen bonds in the last 900 ps are not noticeably influenced by the introduction of dummy atoms, heavy hydrogen atoms, or large time steps.

In Table IV (col. B), a summary is given of the maximum time steps for which a 1-ns simulation could be performed without errors. These time steps are somewhat smaller than those obtained from monitoring the energy drift, as summarized in column A. Because the energy drift was determined from simulations in vacuum, it could be expected that this difference is due to the interactions between protein and water. However, tests of long simulations of the protein in vacuum yield the same maximum time steps as those found for the protein in water. This means that the time-step-limiting-factors arise from the protein and not from the water, as can also be seen from comparison of the maximum time steps found for the water box (see Table II) and for the protein in vacuum (see Table IV).

In Figure 3, interprotein hydrogen-bond distance and angle distributions are shown. It is clear that the introduction of dummy atoms gives rise to slightly broader distributions. This is to be expected, because, for normal hydrogens, the bond angle can adjust itself to accommodate an optimal

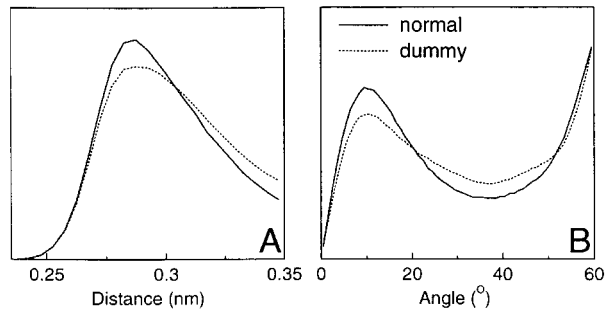

FIGURE 3. Interprotein hydrogen bonds. (A) Donor–acceptor distance distribution and (B) hydrogen donor–acceptor angle distribution, averaged over all simulations without dummy atoms (''normal'') and with dummy atoms (''dummy''). All distributions appear to be insensitive to changes in time step and hydrogen masses.

hydrogen-bonding conformation. Removing this freedom by constructing the hydrogen as a dummy atom makes adjustment impossible, giving rise to more suboptimal hydrogen-bonding conformations and, hence, a slightly broader distribution. In contrast, no effect on the distributions is noticeable from changing hydrogen masses or time step.

In Figure 4, dihedral angle distributions are plotted for the C—NH_3^+ dihedral angle, averaged over time steps (Fig. 4A) and topology types (Fig. 4B). It is clear that neither introduction of dummy atoms in the —NH_3^+ group, nor increase of mass of the hydrogen atoms, nor taking larger time steps has a noticeable effect on the dihedral angle distributions.

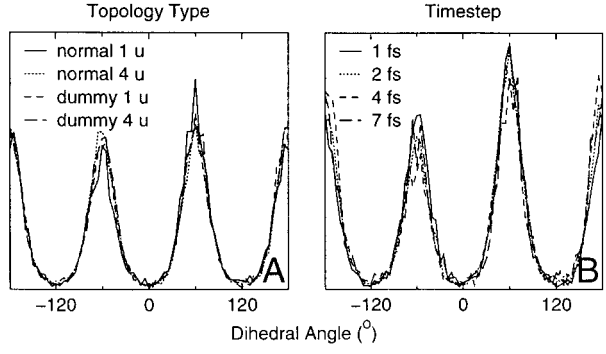

FIGURE 4. Dihedral angle distributions in Lys24—NH_3^+ of the protein. (A) Averaged over all time steps for each topology type. (B) Averaged over topology types for time steps of 1, 2, 4, and 7 fs (see Table III for an overview of simulations at different time steps and topology type).

Discussion and Conclusions

In MD simulations of proteins, in which bond lengths are constrained, the usual time step is 2 fs. This is only slightly below the absolute maximum, which is shown to be 3 fs, the 2-fs maximum being a practical limit imposed by the use of the SHAKE algorithm. To perform simulations at larger time steps, the hydrogen degrees of freedom should be further restricted. This can be done either by defining additional constraints, or by treating hydrogen atoms as ''dummy'' atoms, constructed from neighboring ''real'' atoms. We have chosen the latter approach because it: (i) avoids problems with constraints in planar groups; (ii) allows the combination of two constrained and one flexible angle in a plane (as for the backbone amide proton); and (iii) enables the use of the more stable LINCS constraint algorithm instead of SHAKE to satisfy constraints.

The removal of hydrogen degrees of freedom is not expected to cause a noticeable disturbance in the physical behavior of the system on longer time scales, because the hydrogen motions are almost uncoupled from the main chain vibrations. This stands in contrast to the strongly coupled heavy-atom bond-angle vibrations that influence the accessible configurational space and can therefore not be treated as constraints.[32] Treating all hydrogens as dummy atoms (''dummy 1 u'') allows the time step to be increased by a factor of 2.3 (see Table IV, col. B).

The bottleneck is now the internal rotation or libration of hydrogen-containing groups and of water molecules (see Table I). The frequencies related to such motions will scale inversely proportional to the square root of the moments of inertia and can thus be decreased by modification of the atomic masses. For classical simulations the thermodynamic properties do not depend on the (distribution of) atomic masses. Dynamic properties of a protein on longer time scales will only weakly depend on the mass of hydrogen atoms in the protein, and depend on the properties of water through its bulk transport properties.

Increase of hydrogen mass by a factor of four with simultaneous decrease of the mass of the bonded heavy atom to preserve the total mass of the group (''normal 4 u'') allows for only a modest increase of a factor of 1.3 (see Table IV, col. B). Combining the use of dummies with mass modification (''dummy 4 u'') allows for an increase in time step of 2.3, which is identical to that observed for ''dummy 1 u.'' It appears that no additional gain comes from increasing hydrogen masses in a system in which most hydrogen atoms in the protein are already treated as dummy atoms; however, a gain in simulation stability is to be expected.

The viscosity of water increases and diffusion coefficient decreases by roughly 15%; therefore, the net gain in simulation efficiency can be up to 15% lower than expected based on the increased time step. Additionally, when a neighbor list is used, the efficiency gain will be slightly less; when the neighbor list is to be updated, for example, every 20 fs, counting in integration steps it must be updated more frequently.

Using both dummy atoms and modified masses, the next bottleneck is likely to be formed by the improper dihedrals (which are used to preserve planarity or chirality of molecular groups) and the peptide dihedrals. Although the improper dihedrals could be replaced by dummy-atom constructions, or their potential function modified to reduce the resonance frequencies, the peptide dihedral cannot be changed without affecting the physical behavior of the protein. Thus, we have approached the limit of what can be achieved without affecting the physical behavior.

While we would like to conclude from this discussion that measuring the drift in total energy of a simulation allows one to determine the maximum time step given a maximum order of the drift as a function of the time step, this appears to be not always valid. Table IV (col. A) shows that this criterion would allow for a time step of 3 fs for normal simulation, and an increase by a factor of two for simulating with hydrogen atoms of 4 u. Introducing dummy hydrogens atoms will allow for a gain in the maximum time-step of factor of 2.7, irrespective of the mass of remaining hydrogen atoms. As is evident when comparing columns A and B in Table IV, in real-life examples the maximum time steps will be somewhat lower. It appears that monitoring the total energy drift fails to capture some important features of the simulated system that determine the integration accuracy and stability. This is most pronounced for the ''normal 4 u'' case; based on energy drift, a maximum time step of 6 fs would be expected, but an actual simulation of a protein in water remains stable only up to time steps of 4 fs.

It seems therefore best to choose an important property (or a number of properties) of the system for which a reference value or distribution is

known (either from experiment or from an accurately performed reference simulation), and monitor this property during simulation. This, however, gives rise to a new problem, because, for many systems, such a property might be hard to find.

The most practical approach to determine the maximum time step is simply to determine for which time steps the simulation itself will remain stable. From Table IV, it can be seen that increasing hydrogen atom mass will allow for a modest increase in time step from 3 to 4 fs; however, introducing dummy hydrogen atoms allows the time step to be increased to 7 fs and the combination of increased hydrogen atom mass and dummy hydrogen atoms will give the same time step of 7 fs, but with slightly less fluctuation in certain simulation parameters, and presumably better long-term stability.

Finally, we can say that an increase in time step from 2 to 7 fs, a factor of 3.5, for routine MD simulations of proteins in water, can be achieved by constructing hydrogen atoms in the protein as dummy atoms, leading to a gain in simulation efficiency from a factor of 3 to 3.5. Additional simulation stability can be gained by increasing the mass of all hydrogen atoms with remaining degrees of freedom from 1 to 4 u.

Acknowledgments

The authors thank Dr. M. L. C. E. Kouwijzer for stimulating discussions and A. K. Mazur for some very helpful suggestions. Thanks also go to our undergraduate students for conducting a number of preliminary studies: M. Bergsma, R. M. de Blouw, S. J. Boot, A. Duursma, M. van Faassen, S. Harkema, D. R. Hekstra, M. Mol, and C. Smit.

Appendix: Redistribution of Forces on Dummy Atoms

Dummy atoms are virtual particles with position $\mathbf{r}_d$, which are constructed from the positions of the real particles, $\mathbf{r}_i$. Therefore, every $\mathbf{r}_d$ is a known function of $\mathbf{r}_i$ values. Any force, $\mathbf{F}_d$, on a dummy atom is redistributed to the real atoms on which $\mathbf{r}_d$ depends. When a linear combination of three atoms is used in constructing the dummy atom, the weights for redistributing the forces are equal to those used in the linear combination. This redistribution becomes nontrivial if normalization is used in constructing the dummy atom, as is the case for the dummy types used for aromatic, amide, and amine hydrogens (see Fig. 1B and C).

The force acting on atom i ($\mathbf{F}'_i$) as a result of the force on the dummy atom must be calculated from the partial derivative of the position of the dummy atom with respect to the position of atom i[7]:

$$\mathbf{F}'_{ix} = -\frac{\partial \mathbf{r}_d}{\partial x_i} \cdot \frac{\partial V}{\partial \mathbf{r}_d} = \frac{\partial \mathbf{r}_d}{\partial x_i} \cdot \mathbf{F}_d \tag{6}$$

Here V is the potential energy expressed in positions of real *and* dummy atom positions. Analogous expressions are valid for the y and z component.

For type B (see Fig. 1B), the position of the dummy atom d is calculated from the positions of the constructing atoms i, j, and k as follows:

$$\mathbf{r}_d = \mathbf{r}_i + b\frac{\mathbf{r}_{ij} + a\mathbf{r}_{jk}}{|\mathbf{r}_{ij} + a\mathbf{r}_{jk}|} \tag{7}$$

where $\mathbf{r}_{ij} = \mathbf{r}_j - \mathbf{r}_i$. Using eq. (6) to calculate the redistributed force for atoms i, j, and k yields:

$$\begin{aligned} \mathbf{F}'_i &= \mathbf{F}_d - \gamma(\mathbf{F}_d - \mathbf{F}_1) \\ \mathbf{F}'_j &= (1-a)\gamma(\mathbf{F}_d - \mathbf{F}_1) \\ \mathbf{F}'_k &= a\gamma(\mathbf{F}_d - \mathbf{F}_1) \end{aligned} \qquad \text{where:} \quad \gamma = \frac{b}{|\mathbf{r}_{ij} + a\mathbf{r}_{jk}|}, \quad \mathbf{F}_1 = \frac{\mathbf{r}_{id} \cdot \mathbf{F}_d}{\mathbf{r}_{id} \cdot \mathbf{r}_{id}}\mathbf{r}_{id} \tag{8}$$

For type C (see Fig. 1C) the position is calculated using:

$$\mathbf{r}_d = \mathbf{r}_i + b\cos\alpha\frac{\mathbf{r}_{ij}}{|\mathbf{r}_{ij}|} + b\sin\alpha\frac{\mathbf{r}_\perp}{|\mathbf{r}_\perp|} \qquad \text{where: } \mathbf{r}_\perp = \mathbf{r}_{jk} - \frac{\mathbf{r}_{ij} \cdot \mathbf{r}_{jk}}{\mathbf{r}_{ij} \cdot \mathbf{r}_{ij}}\mathbf{r}_{ij} \tag{9}$$

with corresponding forces, using eq. (6):

$$\begin{aligned} \mathbf{F}'_i &= \mathbf{F}_d - \frac{b\cos\alpha}{|\mathbf{r}_{ij}|}\mathbf{F}_1 + \frac{b\sin\alpha}{|\mathbf{r}_\perp|}\left(\frac{\mathbf{r}_{ij} \cdot \mathbf{r}_{jk}}{\mathbf{r}_{ij} \cdot \mathbf{r}_{ij}}\mathbf{F}_2 + \mathbf{F}_3\right) \\ \mathbf{F}'_j &= \frac{b\cos\alpha}{|\mathbf{r}_{ij}|}\mathbf{F}_1 - \frac{b\sin\alpha}{|\mathbf{r}_\perp|}\left(\mathbf{F}_2 + \frac{\mathbf{r}_{ij} \cdot \mathbf{r}_{jk}}{\mathbf{r}_{ij} \cdot \mathbf{r}_{ij}}\mathbf{F}_2 + \mathbf{F}_3\right) \\ \mathbf{F}'_k &= \frac{b\sin\alpha}{|\mathbf{r}_\perp|}\mathbf{F}_2 \end{aligned}$$

where:

$$\mathbf{F}_1 = \mathbf{F}_d - \frac{\mathbf{r}_{ij} \cdot \mathbf{F}_d}{\mathbf{r}_{ij} \cdot \mathbf{r}_{ij}} \mathbf{r}_{ij},$$

$$\mathbf{F}_2 = \mathbf{F}_1 - \frac{\mathbf{r}_\perp \cdot \mathbf{F}_d}{\mathbf{r}_\perp \cdot \mathbf{r}_\perp} \mathbf{r}_\perp, \qquad (10)$$

$$\mathbf{F}_3 = \frac{\mathbf{r}_{ij} \cdot \mathbf{F}_d}{\mathbf{r}_{ij} \cdot \mathbf{r}_{ij}} \mathbf{r}_\perp$$

and $\mathbf{r}_\perp$ as defined in eq. (9).

References

1. Mazur, A. K. J Comput Phys 1997, 136, 354.
2. Mazur, A. K. J Phys Chem 1998, 102, 473.
3. Ryckaert, J. P.; Ciccotti, G.; Berendsen, H. J. C. J Comput Phys 1977, 23, 327.
4. Hess, B.; Bekker, H.; Berendsen, H. J. C.; Fraaije, J. G. E. M. J Comput Chem 1997, 18, 1463.
5. Berendsen, H. J. C. In: Deuflhardt, P.; Hermans, J.; Leimkuhler, B.; Mark, A.; Reich, S.; Skeel, R. D., eds. Computational Molecular Dynamics: Challenges, Methods, Ideas; Springer-Verlag: Berlin, 1998.
6. Bennet, C. M. J Comput Phys 1975, 19, 267.
7. Berendsen, H. J. C.; van Gunsteren, W. F. In: Barnes, A. J.; Orville-Thomas, W. J.; Yarwood, J., eds. Molecular Liquids: Dynamics and Interactions, NATO ASI C 135. Reidel: Dordrecht, 1984; pp. 475–500.
8. Jacucci, G.; Rahman, A. In: Report on Workshop Methods in Molecular Dynamics—Long Timescale Events; CECAM: Orsay, 1974; pp. 32–40.
9. Wood, D. W. In: Franks, F., ed. Water: A Comprehensive Treatise, Vol. 6; Plenum: New York, 1979; p. 279.
10. Pomès, R.; McCammon, J. Chem Phys Lett 1990, 166, 425.
11. Egberts, E.; Marrink, S. J.; Berendsen, H. J. C. Eur Biophys J 1994, 22, 423.
12. Mao, B.; Maggiora, G.; Chou, K. C. Biopolymers 1991, 31, 1077.
13. Verlet, L. Phys Rev 1967, 34, 1311.
14. van Gunsteren, W. F.; Berendsen, H. J. C. Gromos-87 Manual, Biomos BV: Groningen, 1987.
15. van Buuren, A. R.; Marrink, S. J.; Berendsen, H. J. C. J Phys Chem 1993, 97, 9206.
16. Daura, X.; Oliva, B.; Querol, E.; Avilés, F. X.; Tapia, O. Prot Struct Funct Gen 1996, 25, 89.
17. Miyamoto, S.; Kollman, P. A. J Comput Chem 1992, 13, 952.
18. Gabdoulline, R. R.; Zheng, C. J Chem Phys 1996, 16, 1428.
19. Berendsen, H. J. C.; Postma, J. P. M.; DiNola, A.; Haak, J. R. J Chem Phys 1984, 81, 3684.
20. Berendsen, H. J. C.; Postma, J. P. M.; van Gunsteren, W. F.; Hermans, J. In: Pullman, B., ed. Intermolecular Forces; Reidel: Dordrecht, 1981; pp. 331–342.
21. Lau, K. F.; Alpher, H. E.; Thacher, T. S.; Stouch, T. R. J Phys Chem 1994, 98, 8785.
22. Smith, P. E.; Pettit, B. M. J Chem Phys 1991, 95, 8430.
23. van der Spoel, D.; van Maaren, P. J.; Berendsen, H. J. C. J Chem Phys 1998, 108, 10220.
24. van Nuland, N. A. J.; Hangyi, I. W.; van Schaik, R. C.; Berendsen, H. J. C.; van Gunsteren, W. F.; Scheek, R. M.; Robillard, G. T. J Mol Biol 1994, 237, 544.
25. Hockney, R. W.; Eastwood, J. W. Computer Simulation Using Particles; McGraw-Hill: New York, 1981.
26. Luty, B. A.; Davies, M. E.; Tironi, I. G.; van Gunsteren, W. F. Mol Sim 1994, 14, 11.
27. Berendsen, H. J. C.; van der Spoel, D.; van Drunen, R. Comput Phys Commun 1995, 91, 43.
28. van der Spoel, D.; van Buuren, A. R.; Apol, E.; Meulenhoff, P. J.; Tielman, D. P.; Sijbers, A. L. T. M.; van Drunen, R.; Berendsen, H. J. C. GROMACS User Manual, Version 1.5; Groningen, The Netherlands. http://rugmd0.chem.rug.nl/~gmx, 1997.
29. Allen, M. P.; Tildesley, D. J. Computer Simulations of Liquids; Oxford Science Publications: Oxford, 1987.
30. Berendsen, H. J. C. In: Meyer, M.; Pontikis, V., eds. Computer Simulations in Material Science; Kluwer: Dordrecht, 1991, pp. 139–155.
31. Montrose, C. J.; Bucaro, J.; Marshall-Coakley, J.; Litovitz, T. J Chem Phys 1974, 60, 5025
32. van Gunsteren, W. F.; Berendsen, H. J. C. Mol Phys 1977, 34, 1311.
33. Lide, D. R., ed. CRC Handbook of Chemistry and Physics: A Ready-Reference Book of Chemical and Physical Data, 72nd Ed., CRC Press: Boca Raton, 1991.
34. Kabsch, W.; Sander, C. Biopolymers 1983, 22, 2577.